
CDOT: Continuous Domain Adaptation using Optimal Transport

Guillermo Ortiz Jimenez

EPFL, LTS4, Lausanne, Switzerland
guillermo.ortizjimenez@epfl.ch

Mireille El Gheche

EPFL, LTS4, Lausanne, Switzerland
mireille.elgheche@epfl.ch

Effrosyni Simou

EPFL, LTS4, Lausanne, Switzerland
effrosyni.simou@epfl.ch

Hermine Petric Maretic

EPFL, LTS4, Lausanne, Switzerland
hermine.petricmaretic@epfl.ch

Pascal Frossard

EPFL, LTS4, Lausanne, Switzerland
pascal.frossard@epfl.ch

1 Introduction

The vast majority of machine learning algorithms are designed and built around the assumption that the training and test samples are independent and identically distributed. Nevertheless, in most situations this is not the case, and in practice some type of distributional shift exists between the training and test distributions. And this may cause a significant drop in the performance of any classification method.

Domain adaptation algorithms [1] try to solve this mismatch, and propose ways to design classifiers that can handle differences in the test and trained distribution. The corpora of research in this field is extremely prolific, but in most cases, it has targeted the scenario in which there is access to a large amount of labeled training data from a source domain, but only a set of unlabeled test samples is given from a target domain. In this scenario, it can be shown that the performance of the adaptation depends on the *distance* between the source and target domains. In this sense, optimal transport [2], and its powerful mathematical machinery that defines distances between probability distributions by taking into account the geometry of the underlying space, has been very successful to define a theoretical framework to consider this type of problem.

In this work, we address the scenario in which the target domain is continually, albeit slowly, evolving, and in which, at different time frames, we are given a batch of test data to classify (cf. Figure 1). This type of behaviour can be seen in a variety of applications, such as traffic monitoring with gradually changing lightning and atmospheric conditions [3], spam emails evolving through time, or smooth regional variations of language across a country [4]. Continuous domain adaptation has also found applications in healthcare, adapting the problem of X-ray segmentation to different domains [5].

In particular, we exploit the geometry-awareness that optimal transport offers for the resolution of continuous domain adaptation problems. We propose a regularized optimal transport model that takes into account the transportation cost, the entropy of the probabilistic coupling, the labels of the source domain, and the similarity between successive target domains. The resulting optimization problem is efficiently solved with a forward-backward splitting algorithm based on Bregman distances [6, 7]. Experiments show that the proposed approach leads to a significant improvement in terms of speed and performance with respect to the state of the art [8].

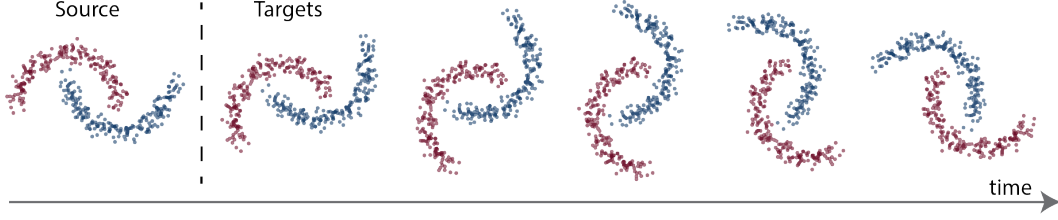


Figure 1: Example of a source domain and a sequence of slowly-varying target domains.

Related work Previous work has addressed the problem of domain adaptation using optimal transport. In [9], Courty *et al.* propose to learn a transportation plan (using a barycentric mapping) that matches the distributions of the two domains, while constraining labelled samples of the same class to remain close during the transportation. This constraint is achieved through a regularization term based on group sparsity or a graph Laplacian matrix. This work is extended in [10], where the authors propose a new formulation to jointly train a classifier while learning the transport plan. To allow for the inclusion of out-of-sample examples, Perrot *et al.* [11] propose to move beyond a barycentric mapping and learn an explicit mapping jointly with the optimal transport objective. This approach was scaled up in [12], where the Monge map is obtained in a two step approach [12] using the dual formulation of the optimal transport problem with entropic regularization. In this sense, they use the OT plan computed in the first step to train a neural network that can be used as an estimation for the Monge map. Finally, Yan *et al.* [13] address the problem of semi-supervised domain adaptation, i.e., when a few labelled examples are given from the target domain, through the use of the Gromov-Wasserstein [14] distance instead of Wasserstein.

To our knowledge, we are the first to tackle the problem of continuous domain adaptation using optimal transport. However, other authors have considered different approaches to solve this problem. Bitarafan *et al.* [15] propose an incremental approach that finds a feature space where source and target data are similarly distributed, so as to classify them in a semi-supervised manner. Bobu *et al.* [16] tackle the problem while ensuring the model continues to correctly classify examples from previous domains, thus avoiding the issue of catastrophic forgetting. Wulfmeier *et al.* train a generative adversarial network to incrementally adapt continuously changing target domains [17].

2 Problem formulation

We denote the available discrete samples by $\{X^{[t]}\}_{0 \leq t \leq M}$, where $X^{[0]} \in \mathbb{R}^{n^{[0]} \times 2}$ is the matrix of the source signal positions, and $\{X^{[t]}\} \in \mathbb{R}^{n^{[t]} \times 2}$ are the matrices of the moving target positions for each time $t \in \{1, \dots, M\}$. We denote the corresponding distributions as $\mu^{[t]} \in \mathbb{R}_+^{n^{[t]}}$, which are embedded in a metric space. As for the optimal transport, we denote as $C^{[t, t+1]} \in \mathbb{R}^{n^{[t]} \times n^{[t+1]}}$ the transport cost between two distributions $\bar{\mu}^{[t]}$ (transported $\mu^{[0]}$ to $\mu^{[t]}$) and $\mu^{[t+1]}$, where each pairwise term $C_{ij}^{[t, t+1]}$ measures the cost to transport the i -th component of $\bar{\mu}^{[t]}$ to the j -th component of $\mu^{[t+1]}$. In addition, we assume that the training samples $X^{[0]}$ are associated with a set of class labels $Y^{[0]} \in \{1, \dots, L\}^{n^{[0]}}$, and the sequence of test samples $\{X^{[t]}\}_{1 \leq t \leq M}$ are associated with unknown labels. Moreover, H_t denotes the entropic regularization defined for every $t \in \{0, \dots, M-1\}$ as

$$(\forall \gamma \in \mathbb{R}^{n^{[t]} \times n^{[t+1]}}) \quad H_t(\gamma) = \sum_{i,j} h(\gamma_{ij}) \quad \text{with} \quad h(\gamma_{ij}) = \begin{cases} \gamma_{ij} \log \gamma_{ij} - \gamma_{ij} & \text{if } \gamma_{ij} > 0 \\ 0 & \text{if } \gamma_{ij} = 0 \\ +\infty & \text{otherwise.} \end{cases} \quad (1)$$

Proposed approach In order to infer the unknown labels $Y^{[t]}$, we propose to estimate the sequential transport plans $\{\gamma^{[t]}\}_{1 \leq t \leq M}$ through the following consecutive steps.

Algorithm 1 Fast algorithm for the regularized optimal transport problem defined in (3).

Require: Function $J_t: \mathbb{R}^{n^{[t]} \times n^{[t+1]}} \rightarrow \mathbb{R}$ with β -Lipschitz continuous gradient

Require: Cost $C^{[t,t+1]} \in \mathbb{R}^{n^{[t]} \times n^{[t+1]}}$, marginals $\mu^{[t]} \in \mathbb{R}^{n^{[t]}}$, and $\mu^{[t+1]} \in \mathbb{R}^{n^{[t+1]}}$

Require: Step-size $\alpha > 0$

Require: Initialization $\gamma_0 \in]0, +\infty[^{n^{[t]} \times n^{[t+1]}}$

- 1: **for** $k = 0, 1, \dots$ **do**
 - 2: $C_k^{[t,t+1]} = \alpha C^{[t,t+1]} + \alpha \nabla J_t(\gamma_k) - \log(\gamma_k)$
 - 3: $\gamma_{k+1} = \text{sinkhorn}(C_k^{[t,t+1]}, 1 + \alpha \lambda, \mu^{[t]} \mu^{[t+1]})$
 - 4: **return** γ_∞
-

1. Firstly, we compute the probabilistic coupling between the source distribution $\mu^{[0]}$ and the first target distribution $\mu^{[1]}$ as the solution to the entropic optimal transport, that is

$$\gamma^{[0]} = \underset{\gamma \in \mathbb{R}^{n^{[0]} \times n^{[1]}}}{\operatorname{argmin}} \langle \gamma, C^{[0,1]} \rangle + \lambda H_0(\gamma) \quad \text{s.t.} \quad \gamma \succcurlyeq 0, \gamma \mathbb{1}^{n^{[1]}} = \mu^{[0]}, \gamma^\top \mathbb{1}^{n^{[0]}} = \mu^{[1]}, \quad (2)$$

where $C^{[0,1]}$ is the transport cost between $\mu^{[0]}$ and $\mu^{[1]}$, $\mathbb{1}^{n^{[t]}} = [1 \dots 1] \in \mathbb{R}^{n^{[t]}}$, and $\lambda > 0$. The regularization H_0 affects the sparsity of $\gamma^{[0]}$, which decreases by setting a higher value for λ , thus leading to a more fuzzy coupling between the source and the target.

2. Then, for every $t \in \{1, \dots, M\}$, we compute the probabilistic coupling between the distribution $\mu^{[t]}$ and the subsequent distribution $\mu^{[t+1]}$ as follows

$$\gamma^{[t]} = \underset{\gamma \in \mathbb{R}^{n^{[t]} \times n^{[t+1]}}}{\operatorname{argmin}} \langle \gamma, C^{[t,t+1]} \rangle + \lambda H_t(\gamma) + \eta_c R_c(\gamma) + \eta_t R_t(\gamma) \quad (3)$$

s.t. $\gamma \succcurlyeq 0, \gamma \mathbb{1}^{n^{[t+1]}} = \mu^{[t]}, \gamma^\top \mathbb{1}^{n^{[t]}} = \mu^{[t+1]},$

where $\eta_c > 0$, $\eta_t > 0$, R_c is the class-based regularizer, and R_t is the time-based regularizer.

- The regularizer R_c aims at conveying a label-based information that is grounded on the assumption that each target sample has to receive masses only from source samples that have the same label [18, 9], yielding

$$R_c(\gamma) = \sum_j \sum_\ell \|\gamma(\mathcal{I}_\ell, j)\|_2. \quad (4)$$

Here above, $\mathcal{I}_\ell \subset \{1, \dots, n^{[t]}\}$ gathers the row indices of $\gamma \in \mathbb{R}^{n^{[t]} \times n^{[t+1]}}$ that belong to the same class $\ell \in \{1, \dots, L\}$. The mixed norm is used in order to model the “group sparsity”, e.g., dependencies between the group of points that belong to the same class.

- R_t aims at enforcing a time varying regularizer, which is modeled through the barycentric mapping¹

$$R_t(\gamma) = \|n^{[t]} \gamma X^{[t]} - n^{[t-1]} \gamma^{[t-1]} X^{[t-1]}\|_F^2. \quad (5)$$

3. Finally, we train a classifier on the mapped source samples $n^{[t-1]} \gamma^{[t-1]} X^{[t-1]}$ and evaluate the accuracy on the new target datapoints $X^{[t]}$.

3 Optimization algorithm

We propose to solve the CDOT problem discribed in the previous section via a forward-backward splitting algorithm based on Bregman distances [6, 7], whose iterations are summarized in Algorithm 1.² To this end, we remark that the Problem (3) can be generically formulated as

$$\underset{\gamma \in \mathcal{S}_t}{\operatorname{minimize}} \quad \varphi_t(\gamma) + J_t(\gamma), \quad (6)$$

¹A barycentric mapping $T_t(X^{[0]})$, of the source signal $X^{[0]}$ to a target signal at time t , is defined by a weighted barycenter of its neighbors in $X^{[t]}$, e.g. $T_t(X^{[0]}) = n^{[t]} \gamma X^{[t]}$.

²In Algorithm 1, $\log(\gamma_k)$ denotes the natural logarithm applied element-wise to the matrix γ_k .

where $J_t: \mathbb{R}^{n^{[t]} \times n^{[t+1]}} \rightarrow \mathbb{R}$ is a differentiable function with β -Lipschitz continuous gradient, $\varphi_t: \mathbb{R}^{n^{[t]} \times n^{[t+1]}} \rightarrow \mathbb{R} \cup \{+\infty\}$ is a lower semicontinuous convex function defined as

$$(\forall \gamma \in \mathbb{R}^{n^{[t]} \times n^{[t+1]}}) \quad \varphi_t(\gamma) = \langle \gamma, C^{[t, t+1]} \rangle + \lambda H_t(\gamma), \quad (7)$$

and $\mathcal{S}_t \subset \mathbb{R}^{N \times N}$ is a convex subset defined as

$$\mathcal{S}_t = \{\gamma \in \mathbb{R}^{n^{[t]} \times n^{[t+1]}} \mid \gamma \succcurlyeq 0, \gamma \mathbb{1}^{n^{[t+1]}} = \mu^{[t]}, \gamma^\top \mathbb{1}^{n^{[t]}} = \mu^{[t+1]}\}. \quad (8)$$

The above problem fits nicely into the forward-backward splitting framework of [6, 7], which allows us to solve (6) through the following iterative algorithm³

$$(\forall k \in \mathbb{N}) \quad \gamma_{k+1} = \text{prox}_{\alpha\varphi_t + \iota_{\mathcal{S}_t}}^f(\nabla f(\gamma_k) - \alpha \nabla J_t(\gamma_k)), \quad (9)$$

where $\gamma_0 \in \mathbb{R}^{n^{[t]} \times n^{[t+1]}}$, $\alpha > 0$, and f is a Legendre function. The key ingredient in the algorithm above is the f -proximity operator of $\varphi_t + \iota_{\mathcal{S}_t}$, which is defined as

$$(\forall \Sigma \in \mathbb{R}^{n^{[t]} \times n^{[t+1]}}) \quad \text{prox}_{\alpha\varphi_t + \iota_{\mathcal{S}_t}}^f(\Sigma) = \underset{\gamma \in \mathcal{S}_t}{\operatorname{argmin}} \alpha\varphi_t(\gamma) + f(\gamma) - \langle \gamma, \Sigma \rangle. \quad (10)$$

By setting $f = H_t$, the proximity operator boils down to an entropic optimal transport problem

$$\text{prox}_{\alpha\varphi_t + \iota_{\mathcal{S}_t}}^{H_t}(\Sigma) = \underset{\gamma \in \mathcal{S}_t}{\operatorname{argmin}} \langle \gamma, \alpha C^{[t, t+1]} - \Sigma \rangle + (1 + \alpha\lambda)H_t(\gamma), \quad (11)$$

whose solution can be efficiently computed with the Sinkhorn algorithm [19]. According to the iterations in (9), replacing Σ with $\nabla H_t(\gamma_k) - \alpha \nabla J_t(\gamma_k)$ leads to Algorithm 1, which is guaranteed to converge to a solution to Problem (6) by adequately setting the step-size α , as discussed in [6, 7].

Note that Algorithm 1 is strikingly similar to the generalized gradient splitting algorithm (CGS) proposed in [8]. Indeed, they both consist of a sequential application of the Sinkhorn algorithm to an initial coupling, until it converges to a solution to the CDOT problem. However, the CGS method performs a line search at each iteration to ensure the convergence, whereas Algorithm 1 simply works with a constant step-size, leading to an optimization method that is both efficient and much easier to implement.

4 Experiments

4.1 Continuous domain adaptation of a rotating distribution

To assess the effectiveness of the proposed time regularization, we compare the adaptation and tracking performance of several optimal transport strategies that use different combinations of regularizers to perform the domain adaptation. In our experiments we replicate the setup proposed in [9] in which they use the standard two entangled moon dataset as source. To create the sequence of targets we sample new data points from the source distribution and rotate them around the origin in batches with steps of 18 degrees. In our simulations we use 500 labeled data samples in the source domain, and 50 samples in each target domain. After each adaptation step, we train a new 1-Nearest Neighbor (1-NN) classifier on the mapped source samples and evaluate its accuracy on a 1000 new datapoints for each target.

We compare three different methods for continuous domain adaptation that use optimal transport. The algorithm proposed in [9], where on top of the typical entropic regularization, they add a group lasso regularization term to the optimal transport problem to penalize transport mappings where samples from different classes in the source are coupled with the same samples in the target. Our proposed algorithm, in which we add the time regularization term introduced in Section 2 to promote temporal smoothness. And finally, a combination of the two algorithms where we add both regularizers in the optimization. Besides, for each of the algorithms we run two sets of experiments:

- **Sequential cost (seq):** We sequentially map the source samples $X^{[0]}$ to the targets at time $t \in \{1, \dots, M\}$. We use the positions of the mapped samples $T_t(X^{[0]})$ and the positions of $X^{[t+1]}$ to compute the optimal transport cost $C^{[t, t+1]} \in \mathbb{R}^{n^{[t]} \times n^{[t+1]}}$.

³ $\iota_{\mathcal{S}_t}$ denotes the indicator function of \mathcal{S}_t , which is equal to 0 for every $\gamma \in \mathcal{S}_t$, and $+\infty$ otherwise.

- **Static cost:** We fix the source samples to $X^{[0]}$ and directly match them to the target samples $X^{[t]}$ at time $t \in \{1, \dots, M\}$. In this case, the transport cost $C^{[0,t]} \in \mathbb{R}^{n^{[0]} \times n^{[t]}}$.

In each set of experiments, we compare three different settings:

- **Time-based regularizer (time reg):** $\lambda = 0.5$, $\eta_t = 50$, and $\eta_c = 0$.
- **Class-based regularizer (class reg):** $\lambda = 0.5$, $\eta_t = 0$, and $\eta_c = 10$.
- **Class-based regularizer + time-based regularizer (class reg + time reg):** $\lambda = 0.5$, $\eta_t = 50$, and $\eta_c = 10$.

Figure 2 shows the performance of the different methods. Clearly, the use of a sequential adaptation strategy, instead of a static one, allows for better tracking and adaptation. Furthermore, we can see that using the previously proposed group lasso regularization on the source labels[18, 9] is not enough to guarantee a continuous adaptation. On the contrary, the time regularizer ensures temporal consistency along the sequence of adaptations and preserves the accuracy of the classification method on all the targets.

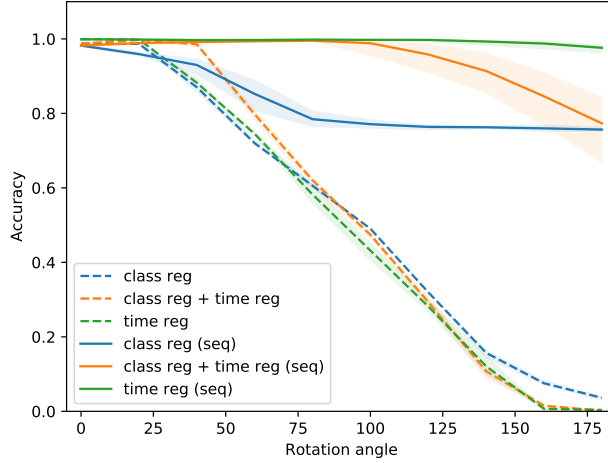


Figure 2: Performance comparison of different continuous domain adaptation strategies with optimal transport. Plot shows average and minimum and maximum values over 10 runs using the best regularization parameters for each of the methods (tuned using grid search on different samples).

Figure 3 illustrates how the source samples are mapped to the targets for a selection of angles (see Appendix 5 for the complete sequence). As we can see, at the beginning of the sequence (cf. Figure 3a) all methods produce similar mappings. However, as the sequence progresses we see that the method that does not use any time regularization fails to produce a consistent continuous mapping and moves all mapped source samples of the same class to a single point in space. On the other hand, adding a time regularization term in the optimization makes sure that the source samples follow the flow of the target distribution and that they are not pulled towards a single center.

4.2 Speed of convergence of the optimization algorithm

We study the performance of the proposed approach on the simulated example discussed in the previous section. The experiments are performed with 5000 samples in the source domain and 1000 in one target domain, using two different sets of regularization parameters. For both Algorithm 1 and CGS algorithm [8], Figure 4 reports the normalized cost evaluations versus the cumulative time per iteration. The curves show that the proposed approach converges faster than CGS, especially with a low entropic regularization (i.e., small λ). This is due to the fact that one iteration of Algorithm 1 is cheaper than one iteration of CGS algorithm, due to the line search performed by the latter to adjust the step size.

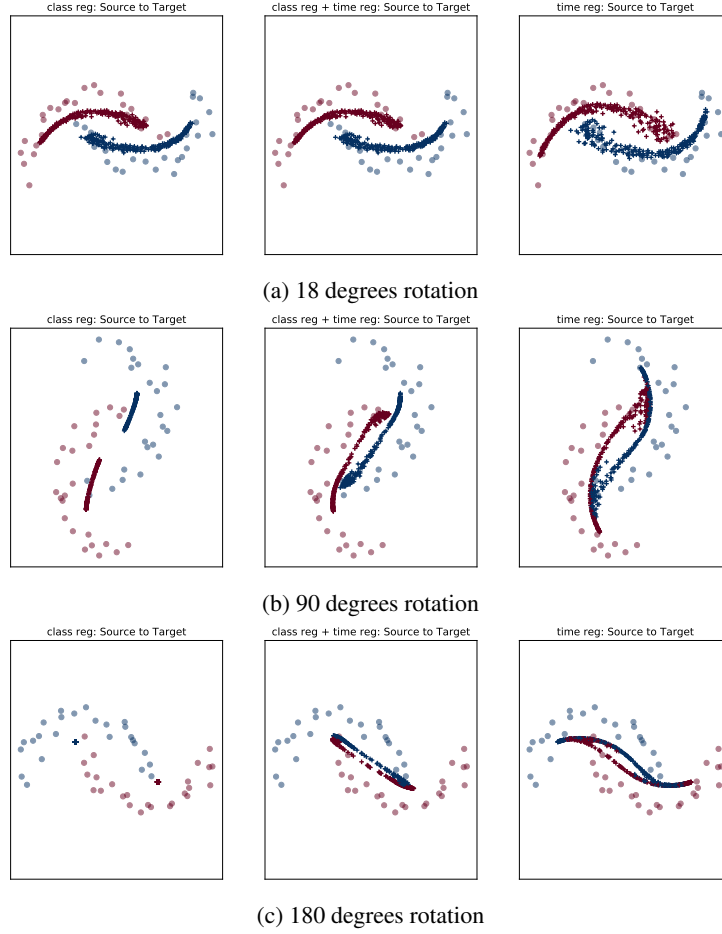
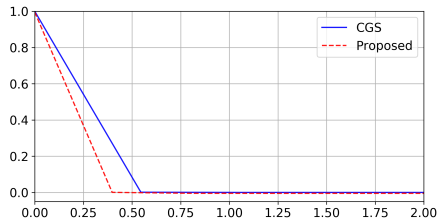
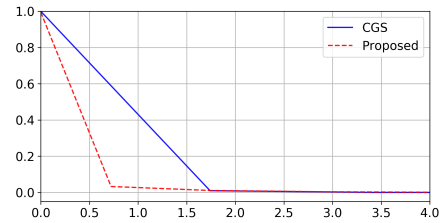


Figure 3: Comparison of mapping estimation on moon dataset for selected angles. Circles represent target samples and crosses source samples mapped to the target.



(a) $\lambda = 0.5$, $\eta_c = 0$, $\eta_t = 50$.



(b) $\lambda = 0.01$, $\eta_c = 0$, $\eta_t = 50$.

Figure 4: Objective value versus time. The step size is set to $\alpha = 10$.

5 Conclusions

We presented an optimal transport based approach to perform continuous domain adaptation on slowly varying target distributions. Our solution is based on the introduction of a new time regularization term to the optimal transport problem that promotes smoothness along the trajectory of the mapped source samples. Furthermore, we proposed a new forward-backward splitting algorithm to solve the optimization problem. Nevertheless, this new algorithm is general enough and it can be used with any form of differentiable regularization placed alongside the standard entropic regularization of optimal transport. Finally, we have tested the our framework on a synthetic example and showed its superior performance over the state-of-the-art algorithms.

References

- [1] M. Wang and W. Deng, “Deep visual domain adaptation: A survey,” *Neurocomputing*, vol. 312, pp. 135–153, Oct. 2018.
- [2] C. Villani, *Optimal transport: old and new*. Springer Science & Business Media, 2008, vol. 338.
- [3] J. Hoffman, T. Darrell, and K. Saenko, “Continuous manifold based adaptation for evolving visual domains,” in *Proceedings of the IEEE Conference on Computer Vision and Pattern Recognition*, 2014, pp. 867–874.
- [4] S. Ruder, P. Ghaffari, and J. G. Breslin, “Towards a continuous modeling of natural language domains,” in *Proceedings of the Workshop on Uphill Battles in Language Processing: Scaling Early Achievements to Robust Methods*, 2016, pp. 53–57.
- [5] R. Venkataramani, H. Ravishankar, and S. Anamandra, “Towards continuous domain adaptation for healthcare,” *arXiv preprint arXiv:1812.01281*, 2018.
- [6] Q. Van Nguyen, “Forward-backward splitting with bregman distances,” *Vietnam Journal of Mathematics*, vol. 45, no. 3, pp. 519–539, 2017.
- [7] M. Bui and P. Combettes, “Bregman forward-backward operator splitting,” *Vietnam Journal of Mathematics*, 2019.
- [8] A. Rakotomamonjy, R. Flamary, and N. Courty, “Generalized conditional gradient: analysis of convergence and applications,” LITIS ; Lagrange ; IRISA, Research Report, Oct. 2015.
- [9] N. Courty, R. Flamary, D. Tuia, and A. Rakotomamonjy, “Optimal transport for domain adaptation,” *IEEE transactions on pattern analysis and machine intelligence*, vol. 39, no. 9, pp. 1853–1865, 2016.
- [10] N. Courty, R. Flamary, A. Habrard, and A. Rakotomamonjy, “Joint distribution optimal transportation for domain adaptation,” in *Advances in Neural Information Processing Systems 30*, I. Guyon, U. V. Luxburg, S. Bengio, H. Wallach, R. Fergus, S. Vishwanathan, and R. Garnett, Eds. Curran Associates, Inc., 2017, pp. 3730–3739.
- [11] M. Perrot, N. Courty, R. Flamary, and A. Habrard, “Mapping estimation for discrete optimal transport,” in *Advances in Neural Information Processing Systems*, 2016, pp. 4197–4205.
- [12] V. Seguy, B. B. Damodaran, R. Flamary, N. Courty, A. Rolet, and M. Blondel, “Large-scale optimal transport and mapping estimation,” *arXiv preprint arXiv:1711.02283*, 2017.
- [13] Y. Yan, W. Li, H. Wu, H. Min, M. Tan, and Q. Wu, “Semi-supervised optimal transport for heterogeneous domain adaptation,” in *International Joint Conference on Artificial Intelligence*, 2018, pp. 2969–2975.
- [14] G. Peyré, M. Cuturi, and S. J., “Gromov-wasserstein averaging of kernel and distance matrices,” in *International Conference on Machine Learning*, ser. Proceedings of Machine Learning Research, M. F. Balcan and K. Q. Weinberger, Eds., vol. 48, New York, New York, USA, 20–22 Jun 2016, pp. 2664–2672.

- [15] A. Bitarafan, M. S. Baghshah, and M. Gheisari, “Incremental evolving domain adaptation,” *IEEE Transactions on Knowledge and Data Engineering*, vol. 28, no. 8, pp. 2128–2141, 2016.
- [16] A. Bobu, E. Tzeng, J. Hoffman, and T. Darrell, “Adapting to continuously shifting domains,” *Workshop track - ICLR 2018*, p. 4, 2018.
- [17] M. Wulfmeier, A. Bewley, and I. Posner, “Incremental adversarial domain adaptation for continually changing environments,” in *2018 IEEE International conference on robotics and automation (ICRA)*. IEEE, 2018, pp. 1–9.
- [18] N. Courty, R. Flamary, and D. Tuia, “Domain adaptation with regularized optimal transport,” in *ECML/PKDD 2014*, ser. LNCS, Nancy, France, Sep. 2014, pp. 1–16.
- [19] M. Cuturi, “Sinkhorn distances: Lightspeed computation of optimal transport,” in *Advances in Neural Information Processing Systems 26*, C. J. C. Burges, L. Bottou, M. Welling, Z. Ghahramani, and K. Q. Weinberger, Eds. Curran Associates, Inc., 2013, pp. 2292–2300.

Appendix: Comparison of all source to target mappings

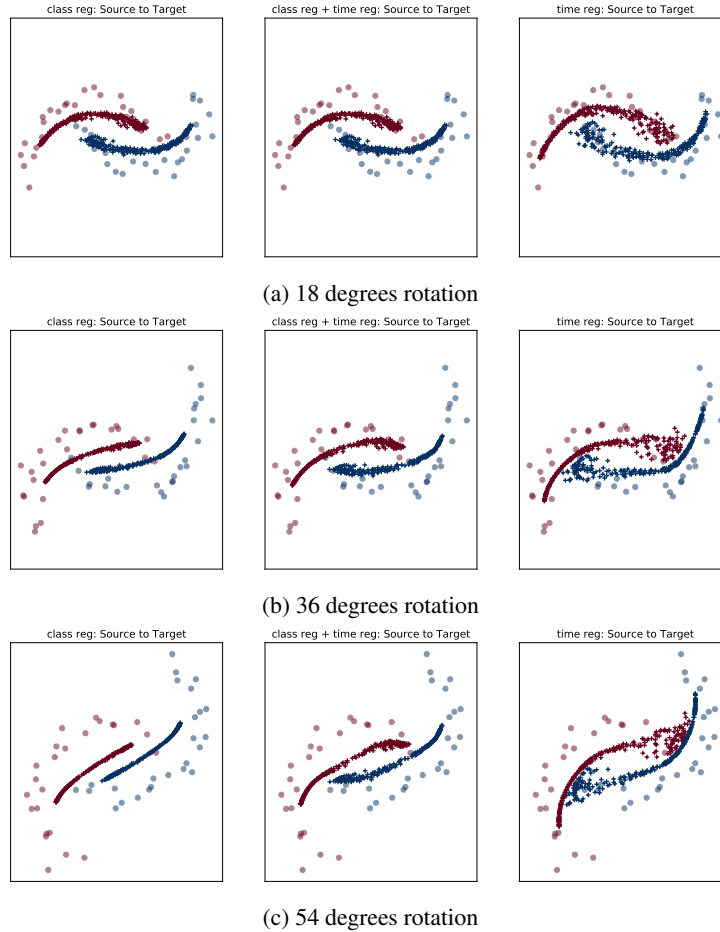


Figure 5: Comparison of mapping estimation on moon dataset. Circles represent target samples and crosses source samples mapped to the target.

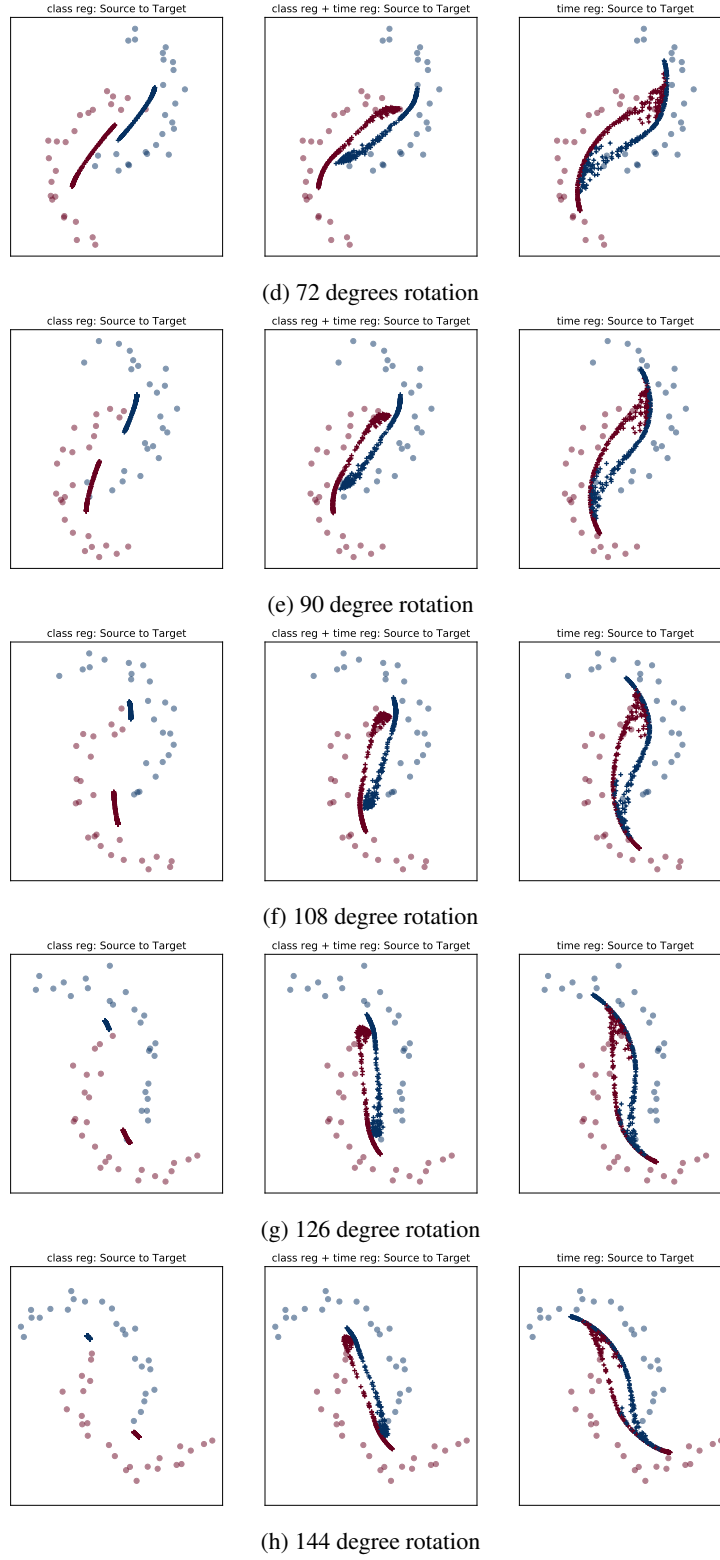


Figure 5: Comparison of mapping estimation on moon dataset. Circles represent target samples and crosses source samples mapped to the target.

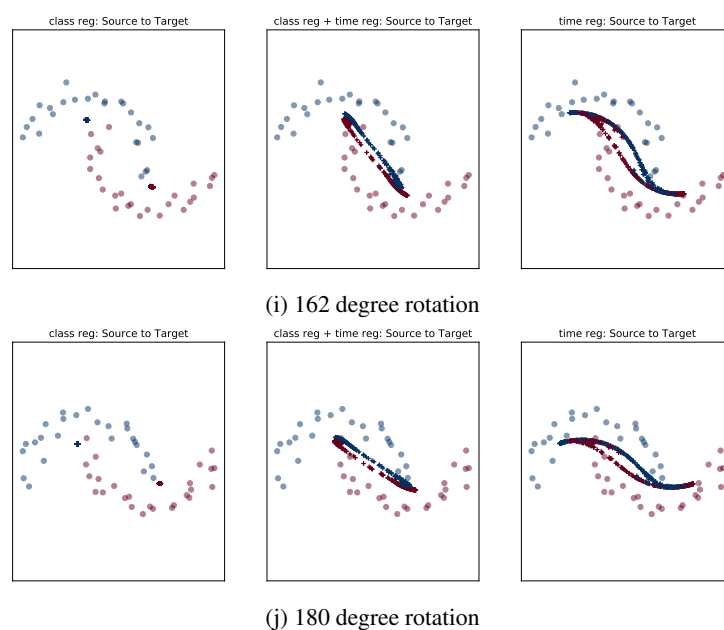


Figure 5: Comparison of mapping estimation on moon dataset. Circles represent target samples and crosses source samples mapped to the target.